

1,1-Dimethylsila-, -germa-, and -stannacycloheptatrienes Fully Annulated with Bicyclo[2.2.2]octene: Syntheses, Structures, and Properties

Tohru Nishinaga, Koichi Komatsu,* and Nobuyuki Sugita

Institute for Chemical Research, Kyoto University, Uji, Kyoto 611, Japan

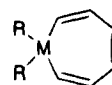
Received November 1, 1994[®]

The titled compounds, i.e., a series of 1,1-dimethyl-2,3:4,5:6,7-tris(bicyclo[2.2.2]octeno)metallacycloheptatrienes (metallepins) containing silicon (**2a**), germanium (**2b**), and tin (**2c**), were synthesized by dilithiation of the terminal dibromide of the linear trimer of bicyclo[2.2.2]octene (**3**) followed by the reaction with $(\text{CH}_3)_2\text{MCl}_2$ ($\text{M} = \text{Si, Ge, Sn}$). The X-ray structure determination was conducted for the first time for these metallepins containing Group 14 elements and indicated that the central seven-membered ring is in a boat-form for all of **2a–c**. As the effective size of the Group 14 metal atom increases, the dihedral angle between the base plane and the stern part of the boat form was found to increase, i.e., the boat structure becomes more deeply folded, for release of the inner angle strain. Variable-temperature NMR measurements indicated that the metallepin ring of **2** is rapidly inverting in solution, and the line-shape analyses gave the activation parameters for ring-inversion at 25 °C as follows: **2a**, $\Delta H^\ddagger = 13.4 \pm 1.3 \text{ kcal mol}^{-1}$, $\Delta S^\ddagger = 3 \pm 5 \text{ cal K}^{-1} \text{ mol}^{-1}$, $\Delta G^\ddagger = 12.4 \pm 0.2 \text{ kcal mol}^{-1}$; **2b**, $\Delta H^\ddagger = 16.0 \pm 1.8 \text{ kcal mol}^{-1}$, $\Delta S^\ddagger = 7 \pm 6 \text{ cal K}^{-1} \text{ mol}^{-1}$, $\Delta G^\ddagger = 14.0 \pm 0.1 \text{ kcal mol}^{-1}$; **2c**, $\Delta H^\ddagger = 21.3 \pm 3.1 \text{ kcal mol}^{-1}$, $\Delta S^\ddagger = 10 \pm 9 \text{ cal K}^{-1} \text{ mol}^{-1}$, $\Delta G^\ddagger = 18.4 \pm 0.5 \text{ kcal mol}^{-1}$. Thus, the energy barrier for ring inversion increases as the carbon–metal bond is elongated, reflecting the increasing instability of the planar transition-state structure due to the inner-angle strain. The larger energy barrier for inversion of **2a** than that of the corresponding cycloheptatriene **6** implies that the cyclic (p–d) π delocalization would not be operating in a planar transition-state structure or negligibly small if present. The UV absorption of **2a**, **2b**, and **2c** (λ_{max} in *n*-hexane 276, 275, and 268 nm, respectively) did not show much difference from that of the C-unsubstituted metallepins **1a**, **1b**, and **1c** in spite of annelation with three bicyclo[2.2.2]octene units, probably because of the more folded boat structure of the central seven-membered ring and less π -conjugation in **2a–c** than in **1a–c**.

Introduction

The fully unsaturated seven-membered heterocycles containing Group 14 elements, metallepins **1**, are of interest from various points of view.^{1–6} Thus, silepins^{1–4} were studied, in search for a possibility of cyclic (p–d) π conjugation,³ for examination of molecular flexibility,^{2b} and also as a possible precursor of a yet unknown

silatropylium ion.^{3b,c,7} Stannepins⁵ have attracted interest as a precursor of borepins.⁸ If the six π -electrons can delocalize over the whole seven-membered ring, the tropylium-ion like stabilization could be expected.



1a, M = Si, R = CH₃

1b, M = Ge, R = CH₃

1c, M = Sn, R = C₃H₇

Recently a series of C-unsubstituted metallepins containing Group 14 elements **1a–c** were reported by Nakadaira et al.⁴ These compounds were considered to have a boat-conformation as judged from the NMR coupling constants of the olefinic ring protons. However, there has been no X-ray structural data reported for any of these or C-substituted metallepins containing Group 14 elements;⁹ the X-ray crystallographic data have so far been limited only to the lattice parameters of a tribenzosilepin derivative.² The energy barrier for ring inversion of silepin is of particular interest with respect to the degree of the possible stabilization by the (p–d) π cyclic conjugation at the planar transition state. However, such data has not been measured yet in spite of several attempts.^{2b,3,4a} The barrier of the tribenzo-derivative was too large^{2b} and that for other derivatives was too small^{3,4a} to be observed by NMR. It is therefore highly desirable

[®] Abstract published in *Advance ACS Abstracts*, February 15, 1995.

(1) (a) Birkofer, L.; Haddad, H. *Chem. Ber.* **1969**, *102*, 432–434; **1972**, *105*, 2101–2103. (b) Birkofer, L.; Haddad, H.; Zamarlik, H. *J. Organomet. Chem.* **1970**, *25*, C57–C58. (c) Corey, J. Y.; Dueber, M.; Bichlmeir, B. *J. Organomet. Chem.* **1971**, *26*, 167–173. (d) Ishikawa, M.; Fuchikami, T.; Kumada, M. *Tetrahedron Lett.* **1976**, 1299–1302. (e) Birkofer, L.; Haddad, H. *Chem. Ber.* **1977**, *110*, 3314–3318. (f) Corey, J. Y.; Farrell, R. L. *J. Organomet. Chem.* **1978**, *153*, 15–23. (g) Ishikawa, M.; Fuchikami, T.; Kumada, M. *J. Organomet. Chem.* **1978**, *162*, 223–238. (h) Birkofer, L.; Haddad, H. *J. Organomet. Chem.* **1979**, *164*, C17–C19.

(2) (a) Andrianof, K. A.; Volkava, L. M.; Derazari, N. V.; Chumaeskii, N. A. *Khim. Geterotskil. Soedin.* **1967**, 435; *Chem. Abstr.* **1967**, *67*, 10869c. (b) Corey, J. Y.; Corey, E. R. *Tetrahedron Lett.* **1972**, 4669–4672.

(3) (a) Cartledge, F. K.; Mollère, P. D. *J. Organomet. Chem.* **1971**, *26*, 175–181. (b) Barton, T. J.; Volz, W. E.; Johnson, J. L. *J. Org. Chem.* **1971**, *36*, 3365–3367. (c) Barton, T. J.; Kippenhan, R. C., Jr.; Nelson, A. J. *J. Am. Chem. Soc.* **1974**, *96*, 2272–2273.

(4) (a) Nakadaira, Y.; Sato, R.; Sakurai, H. *J. Organometallics* **1991**, *10*, 435–442. (b) Nakadaira, Y.; Sato, R.; Sakurai, H. *J. Organomet. Chem.* **1992**, *441*, 411–417.

(5) (a) Leusink, A. J.; Noltes, J. G.; Budding, H. A.; van der Kerk, G. J. M. *Recl. Trav. Chim. Pays-Bas.* **1964**, *83*, 1036–1038. (b) Leusink, A. J.; Budding, H. A.; Noltes, J. G. *J. Organomet. Chem.* **1970**, *24*, 375–386.

(6) Corey, J. Y.; Deuber, M.; Malaidza, M. *J. Organomet. Chem.* **1972**, *36*, 49–60.

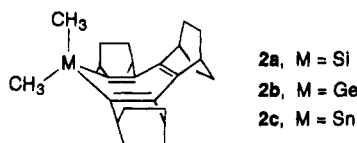
(7) Olah, G. A.; Rasul, G.; Heiliger, L.; Bausch, J.; Prakash, G. K. S. *J. Am. Chem. Soc.* **1992**, *114*, 7737–7742.

(8) Sugihara, Y.; Yagi, T.; Murata, I. *J. Am. Chem. Soc.* **1992**, *114*, 1479–1481, and the leading references cited therein.

(9) An X-ray structural analysis of the metallepin has only been reported for Sb–chlorobenzod]stibepin: Ashe, A. J., III; Goossen, L.; Kampf, J. W.; Konishi, H. *Angew. Chem., Int. Ed. Engl.* **1992**, *31*, 1642–1643. Also the previous works on the heterepins containing Group 15 and 16 elements are surveyed therein.

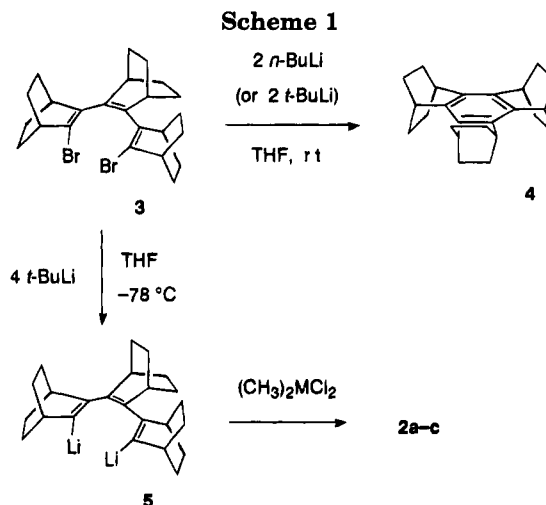
to determine the X-ray structures for a series of metallepins with completely the same substituents and also to examine their dynamic behavior such as ring inversion.

In our previous study we prepared a series of cyclic π -conjugated systems annelated with a rigid bicyclic σ -framework, i.e., bicyclo[2.2.2]octene, and demonstrated the presence of effective σ - π conjugation between the 2p orbital and the rigidly held σ -bonds.¹⁰ In particular, the full annelation with bicyclo[2.2.2]octene was found to cause remarkable stabilization of the tropylium ion.^{10a} Such a structural modification was also found to be advantageous in growth of single crystals owing to the presence of highly symmetrical structural units.¹¹ Thus we synthesized a series of 1,1-dimethylmetallacycloheptatrienes (1,1-dimethylmetallepins) fully annelated with bicyclo[2.2.2]octene, containing silicon (**2a**), germanium (**2b**), and tin (**2c**), and investigated their structure and properties. The results are reported here in detail.



Results and Discussion

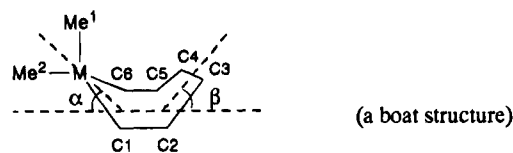
Synthesis. Previously, we synthesized the terminal dibromide of bicyclo[2.2.2]octene trimer (**3**) by linear trimerization of the bicyclic units initiated by monolithiation of 2,3-dibromobicyclo[2.2.2]octene with *n*-BuLi in THF at -78°C , which involved repeated formation of bicyclo[2.2.2]octyne, its insertion into the precursor's C-Li bond, and Li/Br exchange.^{10b} Further reaction of dibromide **3** with 2 equiv of *n*-BuLi in THF at room temperature resulted in cyclization to benzene derivative **4**. This reaction was supposed to proceed via a σ -radical formed by dissociative electron-transfer.¹² In contrast, treatment of **3** with 4–5 equiv of *t*-BuLi in THF at -78°C resulted in the formation of dilithiated compound **5**, which was then allowed to react with dichlorodimethylsilane, -germane, and -stannane to give the desired metallepins **2a**, **2b**, and **2c** as shown in Scheme 1.¹³ The same reaction, when carried out at room temperature, resulted in cyclization to benzene **4**. Purification of **2a**, **2b**, and **2c** was attained only by recrystallization after removal of most of byproducts by passing through a



column of alumina. The isolated yield of the purified product was 44% for **2a**, 28% for **2b** and 17% for **2c**.

These metallepins **2a–c** were stable in solid state but readily decomposed under even slightly acidic conditions, for example, in chloroform solutions or during elution from a silica-gel column. The relatively low yield of **2c** is apparently due to its instability reflecting the weakest carbon–metal bond among the three. In fact, stannepin **2c** decomposed to benzene **4** when it was heated in nitrobenzene-*d*₅ at 110°C ($t_{1/2} = 41\text{ min}$),¹⁴ whereas no such structural change was observed for **2b** and **2c** under the same conditions.

X-ray Structures. The X-ray crystallographic analysis was performed for the single crystals of the metallepins **2a–c**, which were grown by slow diffusion of acetonitrile into the solution in benzene. As shown by the ORTEP views in Figure 1, all of these compounds have a quite similar structure with the central seven-membered ring in a boat form. The selected X-ray structural parameters of these compounds are summarized in Table 1. Apparently, the most notable difference in their structures is the M–C1 bond length. As the atomic radii of the Group 14 elements increases, the M–C1 bond is elongated while the lengths of the rest of the triene-part of the seven-membered ring remain essentially the same.



As to the bond angles in the central seven-membered ring, no significant difference was observed except for the angle C1–M–C6. On the other hand, appreciable difference was observed for the bent angles in the boat

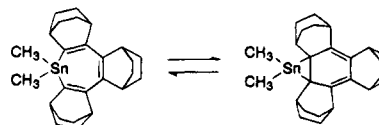
(10) (a) Komatsu, K.; Akamatsu, H.; Jinbu, Y.; Okamoto, K. *J. Am. Chem. Soc.* **1988**, *110*, 633–634. (b) Komatsu, K.; Aonuma, S.; Jinbu, Y.; Tsuji, R.; Hirose, C.; Takeuchi, K. *J. Org. Chem.* **1991**, *56*, 195–203. (c) Aonuma, S.; Komatsu, K.; Takeuchi, K. *Chem. Lett.* **1991**, 767–770. (d) Komatsu, K.; Akamatsu, H.; Aonuma, S.; Jinbu, Y.; Maekawa, N.; Takeuchi, K. *Tetrahedron* **1991**, *47*, 6951–6766. (e) Komatsu, K. *Pure Appl. Chem.* **1993**, *65*, 73–80.

(11) (a) The benzene derivative: Komatsu, K.; Jinbu, Y.; Gillette, G. R.; West, R. *Chem. Lett.* **1988**, 2029–2032. (b) The cyclooctatetraene derivative: Komatsu, K.; Nishinaga, T.; Aonuma, S.; Hirose, C.; Takeuchi, K.; Lindner, H. J.; Richter, J. *Tetrahedron Lett.* **1991**, *32*, 6767–6770. (c) A cation radical of the cyclooctatetraene derivative: Nishinaga, T.; Komatsu, K.; Sugita, N.; Lindner, H. J.; Richter, J. *J. Am. Chem. Soc.* **1993**, *115*, 11642–11643. (d) The tropylium ion derivative: Kagayama, A.; Komatsu, K.; Nishinaga, T.; Takeuchi, K.; Kabuto, C. *J. Org. Chem.* **1994**, *59*, 4999–5004. (e) The cyclopentadiene derivative: Komatsu, K.; Nishinaga, T.; Takeuchi, K.; Lindner, H. J.; Richter, J. *J. Org. Chem.* **1994**, *59*, 7322–7328.

(12) Andrieux, C. P.; Merz, A.; Savéant, J.-M. *J. Am. Chem. Soc.* **1985**, *107*, 6097–6103 and references are cited therein. See also Garst, J. F.; Barbas, J. T. *J. Am. Chem. Soc.* **1974**, *96*, 3239–3246.

(13) An attempted dilithiation by the use of *n*-BuLi at -78°C was not successful, affording an inseparable complex mixture.

(14) It is supposed that dimethylstannylene, $(\text{CH}_3)_2\text{Sn}$, was split off through the metallacycloheptatriene \rightleftharpoons metallanorcaradiene equilibrium shown below. Similar cleavage was observed for the case of silylene derivative: ref 3b. However, the fate of $(\text{CH}_3)_2\text{Sn}$ was not clarified even by careful examination of the product mixture. The rate of formation of benzene **4** was estimated from the change in ^1H NMR spectrum: the rate followed the first-order kinetics and the rate constant was $2.8 \times 10^{-4}\text{ s}^{-1}$.



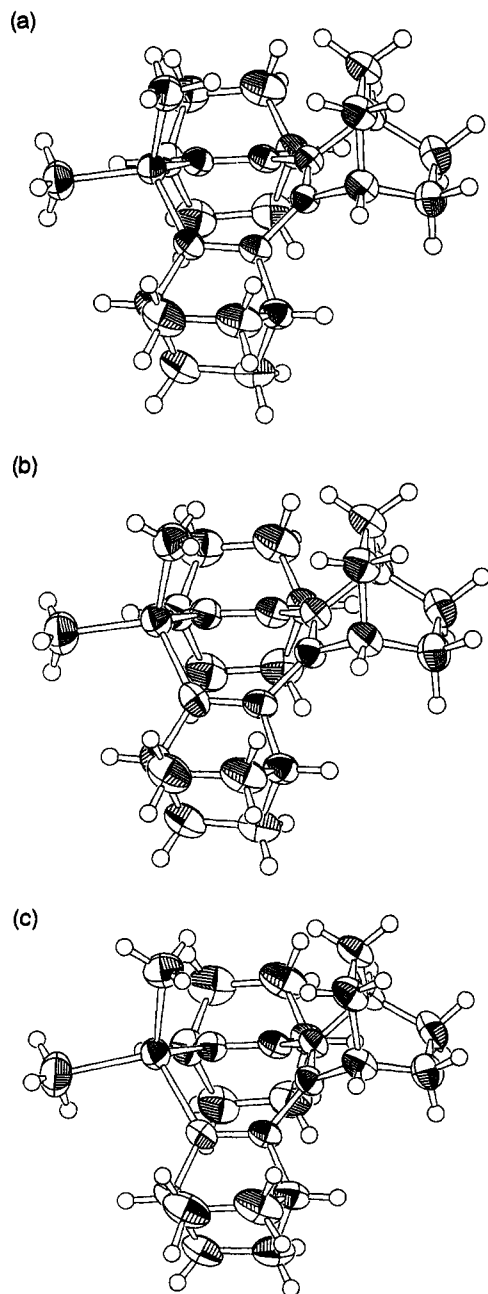
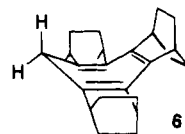


Figure 1. ORTEP views of the X-ray crystal structures of (a) **2a**, (b) **2b**, and (c) **2c** (50% probability).

structure, i.e., the angle α between the base plane (C1–C2–C5–C6) and the bow (C1–M–C6) and the angle β between the base plane and the stern (C2–C3–C4–C5). With the increase in the M–C1 bond length, the angle C1–M–C6 decreases and the boat form becomes more folded as is shown by the increase in the angle β . The results of PM3 semiempirical molecular orbital calculations¹⁵ showed the same tendency as the observed values for the angles C1–M–C6 and β as shown in Table 1. These results are ascribable to the release of the inner angle strain in the central seven-membered ring. On the other hand, the observed α value, which should also be correlated with the β value in principle, exhibited relatively small change in the reverse direction; the change in α value obtained from PM3 calculations is also quite small. This discrepancy may be attributed to the crystal packing effect.

The unit cells of the crystals **2a**, **2b**, and **2c** are all orthorhombic (the space group P_{nma}). Reflecting the similarity in their molecular structures, the mode of crystal packing of all three compounds is the same as exemplified by the packing of **2c** shown in Figure 2. The most notable difference in the lattice constants was observed in the length of a -axis (see the Experimental Section). Since the C1–M–C6 plane and the CH₃–M–CH₃ plane are placed nearly parallel to the ab -plane and ac -plane, respectively, a gradual increase in C–M bond length is reflected in lengthening of the a -axis most pronouncedly.

Dynamic Behaviors. Although the structures of **2a–c** were found to be similar in the solid state, their behavior in solution was quite different with each other. In the ¹H NMR spectra (270 MHz) taken at room temperature, the signal of methyl protons of **2a** exhibited a sharp singlet peak as shown in Figure 3a. However, the signal of the methyl protons of **2b** showed a broad single peak (Figure 3b) and that of **2c** was split into two separate peaks of equal intensity (Figure 3c). These results clearly demonstrate that the boat structure of **2a** is inverting rapidly but that of **2c** is fixed at room temperature in an NMR time-scale. The line shape analyses of the two-site exchange provided the activation parameters at 25 °C as summarized in Table 2. For the purpose of comparison, the data of the cycloheptatriene fully annelated with bicyclo[2.2.2]octene (**6**)¹⁶ are also included.



The ring inversion of the seven-membered ring of the boat form would proceed most probably via a planar structure B in the transition state as shown in Scheme 2. This was supported for the case of unsubstituted cycloheptatriene by ab initio molecular orbital calculations¹⁷ and also for the tris(bicyclo[2.2.2]octeno) derivative **6** by molecular mechanics calculations.¹⁶ Then, the PM3 calculations were carried out to obtain the heat of formation (ΔH_f°) for both the boat structure and the structure with the seven-membered ring fixed at a planar geometry for **2a–c** and **6**, and their difference ($\Delta\Delta H_f^\circ$) was examined. The values of $\Delta\Delta H_f^\circ$ of **2a–c** and **6** were in fair agreement with the observed ΔH^\ddagger values as shown in Table 2, thus supporting the planarity of the seven-membered ring at the transition state of the ring inversion of **2a–c**.

As shown by the ΔG^\ddagger data in Table 2, the barrier for ring inversion increases upon going from cycloheptatriene **6** to metallepins **2a–c** and also as the atomic size of the Group 14 element of metallepins increases. This is primarily attributed to the increase in strain in the planar structure at the transition state: the larger strain is generated by elongation of the C1–M bond that demands widening of inner angles in the planar seven-membered ring. The possibility of cyclic (p–d) π delocal-

(15) MOPAC 6.0.

(16) Aonuma, S.; Komatsu, K.; Takeuchi, K. *Chem. Lett.* **1989**, 2107–2110.

(17) Schulman, J. M.; Disch, R. L.; Sabio, M. L. *J. Am. Chem. Soc.* **1982**, *104*, 3785–3788.

Table 1. Observed and Calculated Bond Lengths, Bond Angles, and Bent Angles of the Central Ring in **2a–2c**

compd	bond length, Å						bond angle, deg				bent angle, deg ^a		
	M–Me ¹	M–Me ²	M–C1	C1–C2	C2–C3	C3–C4	C1–M–C6	M–C1–C2	C1–C2–C3	C2–C3–C4	α	β	
2a	obsd	1.875(4)	1.869(4)	1.857(2)	1.350(3)	1.461(3)	1.363(4)	103.2(1)	120.6(2)	126.6(2)	128.3(1)	45.7	32.7
	calcd ^b	1.900	1.899	1.831	1.351	1.442	1.356	104.3	122.8	126.9	127.9	40.3	33.4
2b	obsd	1.940(6)	1.940(6)	1.926(3)	1.346(4)	1.474(4)	1.359(6)	102.0(2)	120.2(2)	127.2(3)	128.5(2)	44.8	33.5
	calcd ^b	1.976	1.972	1.901	1.344	1.451	1.356	96.6	122.5	126.8	128.2	40.4	35.6
2c	obsd	2.135(9)	2.145(9)	2.108(9)	1.337(7)	1.484(6)	1.350(9)	97.9(4)	119.5(4)	127.4(4)	129.5(2)	43.1	36.7
	calcd ^b	2.119	2.114	2.092	1.347	1.456	1.354	93.4	121.0	125.9	128.5	41.3	40.6

^a Defined in the text. ^b PM3 calculations.

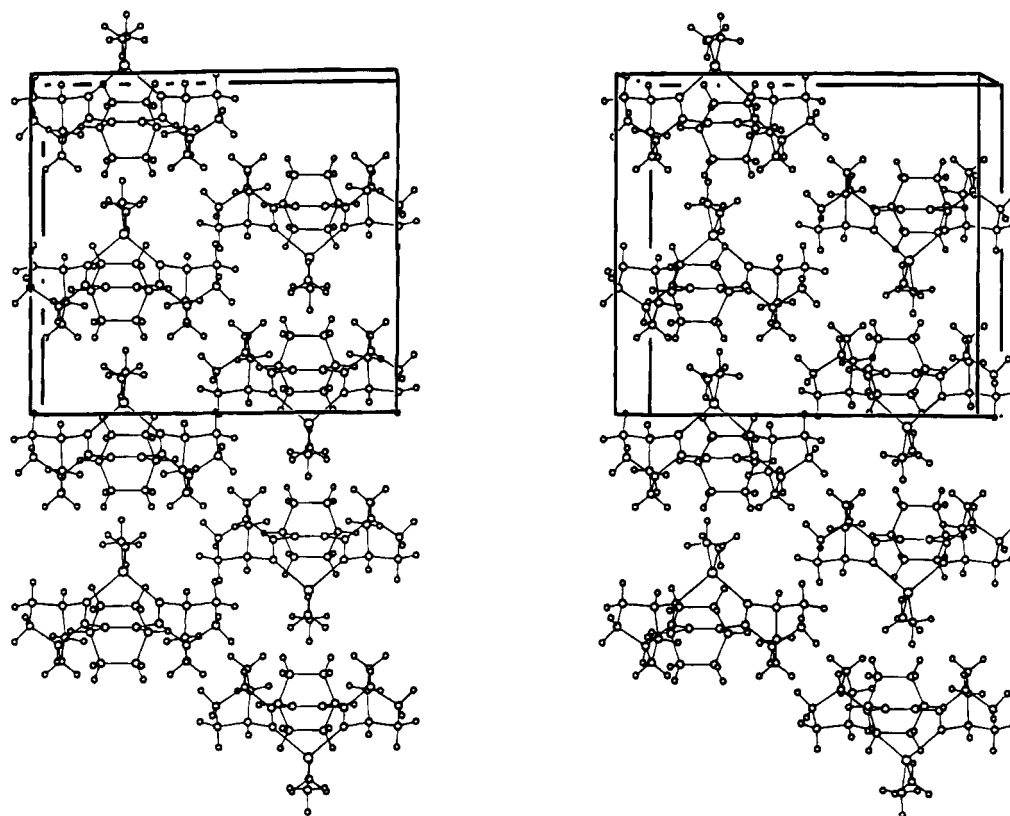


Figure 2. Stereoview of the crystal packing of **2c**. The α -axis points vertically downward, b from left to right, and c toward the reader.

ization in silepins has once attracted some interest.³ If such electronic state is actually contributing to the planar form of **2a**, the inversion barrier should have been appreciably lowered. The observed larger value of ΔG^\ddagger (and of ΔH^\ddagger) of **2a** than that of **6** as shown in Table 2 implies that such an effect would not be operating or negligibly small if present.

Electronic Spectrum. For the case of C-unsubstituted metallepins **1a**, **1b**, and **1c**, the longest-wavelength UV absorption corresponding to the π - π^* transition was reported as 281, 279, and 279 nm, respectively, in *n*-hexane. The bathochromic shift of the absorption of silepin **1a** as compared with that of unsubstituted cycloheptatriene **7** (261 nm) was ascribed to the possible cyclic σ - π conjugation involving the Si-C_{methyl} σ -bonds⁴ and not to the cyclic (p-d) π delocalization mentioned above.³

On the other hand, the metallepins in the present work, **2a**, **2b**, and **2c**, were found to absorb at 276, 275, and 268 nm, respectively, in *n*-hexane. The absorption of silepin **2a** in ethanol is identical to that in *n*-hexane, and, in sharp contrast to the case of silepin **1a** (see above), **2a** did not show any bathochromic shift as compared with the absorption of corresponding cycloheptatriene **6** (λ_{\max} 276 nm in ethanol).¹⁶ The absorption of

6 is bathochromically shifted as compared with the parent cycloheptatriene **7** due to the annelation with three bicyclo[2.2.2]octene units, which raise the HOMO of the π -system by inductive and σ - π conjugative effects and thereby lower the π - π^* transition energy. Then the similar effects may be expected to cause some bathochromic shift for the metallepins **2a–c** as compared with absorptions of **1a–c**. However, experimentally no such shift was observed at all as described above. The most conceivable reason for the absence of such shift is the less effective π -conjugation in the triene part of the seven-membered ring due to the more folded structure in **2a–c** than in **1a–c**: the observed value for β of the seven-membered ring in **2a–c** is 32.7–46.7° (Table 1), while the β value for **1a**, **1b**, and **1c** was estimated as 25°, 26°, and 27°, respectively, from the ¹H NMR coupling constants.⁴ This interpretation is supported by slight hypsochromic shift observed upon going from **2a** to **2c** with the boat structure becoming more deeply folded. The effect of the cyclic σ - π conjugation involving the Si-C_{methyl} σ -bonds in **2a** seems to be counterbalanced by the less effective π -conjugation in the triene part in comparison with **6**.

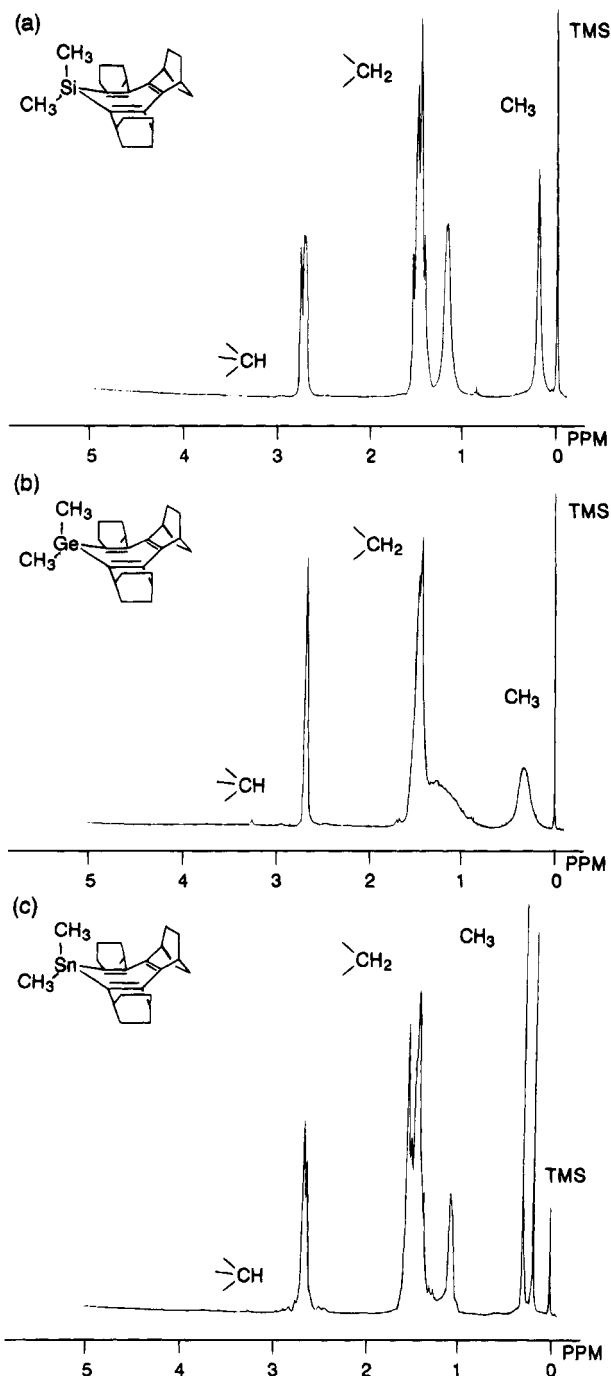


Figure 3. ^1H NMR spectra (270 MHz; C_6D_6) of (a) **2a**, (b) **2b**, and (c) **2c**, at room temperature.

Table 2. Activation Parameters (25 °C) for the Ring Inversion and Calculated $\Delta\Delta H_f$ of **2a–c** and **6**

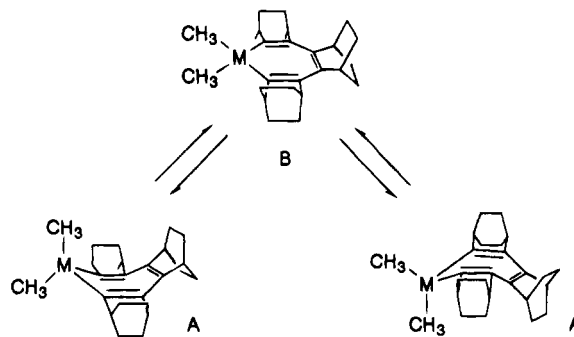
compd	ΔH_f^a	ΔS_f^b	ΔG_f^a	$\Delta\Delta H_f^{a,c}$
6 ^d	7.9 ± 0.5	-11 ± 3	11.3 ± 0.2	6.0
2a	13.4 ± 1.3	3 ± 5	12.4 ± 0.2	10.0
2b	16.0 ± 1.8	7 ± 6	14.0 ± 0.1	10.1
2c	21.3 ± 3.1	10 ± 9	18.4 ± 0.5	17.0

^a In kcal mol⁻¹. ^b In cal K⁻¹ mol⁻¹. ^c $\Delta H_f(\text{planar}) - \Delta H_f(\text{boat})$ by PM3 calculations. ^d Data from ref 16.

Summary

A previously reported technique of cyclization of the bicyclo[2.2.2]octene trimer was modified and applied for the syntheses of a series of metallepins fully annelated with bicyclo[2.2.2]octene units, **2a–c**. The X-ray struc-

Scheme 2



ture determination was conducted for these metallepins for the first time and revealed that their structure is a boat form with the seven-membered ring folded deeper with an increase in the size of the metal atom. The dynamic NMR study on metallepins **2a–c** quantitatively substantiated the notable effect of the carbon–metal bond length upon the relative stability of a planar transition-state structure for the ring inversion. Metallepins **2a–c** are considered to have the deeply folded structure also in solution, similar to that determined by X-ray crystallography, as judged from the electronic spectra. The present study clearly demonstrated that the structural modification such as annelation with the bicyclo[2.2.2]octene units is quite advantageous in the structural analysis of the conjugated cyclic π -system both in solid state and in solution.

Experimental Section

General Procedures. Melting points were determined on a Yamato MP-21 apparatus and are uncorrected. Elemental analyses were performed by Microanalytical Center, Kyoto University, Kyoto. NMR spectra were recorded on Varian XL-300 (300 MHz for ^1H and 75.4 MHz for ^{13}C NMR), on JEOL GSX270 (270 MHz for ^1H and 67.8 MHz for ^{13}C NMR), or on JEOL FX90 (90 MHz for ^1H and 22.5 MHz for ^{13}C NMR) spectrometers using Me_4Si as an internal standard unless otherwise noted. IR spectra were taken on Perkin Elmer 1640 spectrometer. UV-vis spectra were taken on Shimadzu UV-2100PC spectrometer. The PM3 calculations were conducted using the standard methods as implemented in the MOPAC 6.0 semiempirical molecular orbital package on a CRAY Y-MP2E/264 machine.

THF was freshly distilled from sodium benzophenone ketyl before use. A pentane solution of *t*-BuLi was titrated using the THF solution of *N*-pivaloyl-*o*-toluidine.¹⁸ The dibromide of bicyclo[2.2.2]octene trimer **3** was prepared as reported previously.^{10b}

1,1-Dimethyl-2,3:4,5:6,7-tris(bicyclo[2.2.2]octeno)silacycloheptatriene (2a). To a stirred solution of **3** (53.1 mg, 0.111 mmol) in THF (5 mL) at -78°C was added dropwise a solution of 1.5 N *t*-BuLi in pentane (0.37 mL, 0.55 mmol). Addition of each drop of *t*-BuLi solution caused yellow coloration indicative of formation of dilithiated compound **5**. After stirring for 15 min at -78°C , dichlorodimethylsilane (0.13 mL, 142 mg, 1.1 mmol) was added dropwise to the reaction mixture, which gradually turned colorless. After being stirred for 30 min at -78°C , the mixture was warmed to room temperature over 10 min. The solvent was then removed by evaporation, and the crude product was purified by chromatography over alumina eluted with hexane to give **2a** (18.3 mg, yield 43.8%) as a white solid. A single crystal for X-ray analysis was grown by slow diffusion of acetonitrile into a benzene solution: mp $187\text{--}188^\circ\text{C}$ dec; ^1H NMR (270 MHz, C_6D_6 , 25°C) δ 2.77 (br s, 6H), 1.59 (br m, 16H), 1.20 (br s, 8H), 0.20 (s, 6H); this signal split into two peaks at δ 0.41 (3H) and -0.20 (3H) when

measured in THF-*d*₈ at -70 °C with the frequency of 90 MHz¹⁹); ¹³C NMR (67.8 MHz, C₆D₆, 25 °C) δ 150.2, 141.2, 140.8, 33.8, 33.0, 32.9, 26.7, 26.5, 25.7, -3.5 (at -80 °C in THF-*d*₈ with 22.5 MHz frequency, this signal split into two signals at δ -2.8 and -4.5²⁰); IR (KBr) 2945, 2855, 1531, 1453, 1251, 1239, 1160, 1076, 1020, 867, 847, 812, 766, 728, 642 cm⁻¹. Anal. Calcd for C₂₆H₃₆Si: C, 82.91; H, 9.63. Found: C, 82.78; H, 9.69.

1,1-Dimethyl-2,3:4,5:6,7-tris(bicyclo[2.2.2]octeno)germacycloheptatriene (2b). In the same manner as described above for the synthesis of **2a**, dibromide **3** (99.6 mg, 0.208 mmol) was dilithiated and treated with dichlorodimethylgermane (0.12 mL, 191 mg, 1.1 mmol) in THF (10 mL) at -78 °C. After being stirred for 30 min at -78 °C, the mixture was warmed to room temperature, evaporated under reduced pressure, and extracted with benzene (2 mL × 3). The residue from evaporation of the extract was then washed thoroughly with *n*-hexane, and the hexane washings purified by passing through an alumina column to give **2b** (24.3 mg, 27.7%) as colorless crystals after recrystallization from acetonitrile-benzene. A single crystal was grown as described above: mp 280–282 °C dec (sealed tube); sublimes at about 200 °C; ¹H NMR (270 MHz, C₆D₆, 25 °C) δ 2.75 (br s, 6H), 1.6–0.9 (br m, 24H), 0.3 (br s, 6H); this signal split into two peaks at δ 0.37 (3H) and -0.05 (3H) when measured in THF-*d*₈ at -50 °C with the frequency of 90 MHz¹⁹); ¹³C NMR (67.8 MHz, C₆D₆, 25 °C) δ 148.3, 142.6, 140.9, 34.0, 33.5, 33.2, 27–25 (br) (the methyl carbons were not observed at this temperature due to broadening, and were observed at -50 °C in THF-*d*₈ with 22.5 MHz frequency as two signals at δ -2.3 and -6.9²⁰); IR (KBr) 2946, 2857, 1552, 1467, 1453, 1224, 1144, 1017, 867, 810, 602 cm⁻¹. Anal. Calcd for C₂₆H₃₆Ge: C, 74.15; H, 8.62. Found: C, 73.86; H, 8.42.

1,1-Dimethyl-2,3:4,5:6,7-tris(bicyclo[2.2.2]octeno)stannacycloheptatriene (2c). Similarly, dibromide **3** (101 mg, 0.211 mmol) was dilithiated and treated with dichlorodimethylstannane (220 mg, 1.00 mmol) in THF (9 mL) at -78 °C. After being stirred for 30 min at -78 °C, the reaction mixture was warmed to room temperature and evaporated. The crude product was purified by chromatography over alumina and recrystallization by slow diffusion of acetonitrile to the benzene solution, repeated twice, to give **2c** (17.0 mg, 17.2%) as colorless crystals. A single crystal was grown as described above: mp >285 °C; ¹H NMR (270 MHz, C₆D₆, 25 °C) δ 2.70 (br s, 6H), 1.6–1.1 (br m, 24H), 0.31 (s, 3H), 0.19 (s, 3H); ¹³C NMR (67.8 MHz, C₆D₆) δ 151.7, 144.5, 141.9, 35.7, 34.4, 33.6, 27.4, 27.2, 26.8, 25.9, 25.6, 25.5, -8.6, -14.2; IR (KBr) 2912, 2856, 1557, 1451, 1330, 1179, 1153, 1015, 868, 809 cm⁻¹. Anal. Calcd for C₂₆H₃₆Sn: C, 66.83; H, 7.77. Found: C, 67.22; H, 7.72.

X-ray Crystallography on 2a–c.²¹ Data for compounds **2a–c** were collected on a Rigaku AFC7R diffractometer with graphite monochromated Cu Kα radiation and a 12 kW rotating anode generator. Crystal data for **2a** are as follows:

(19) The chemical shift was corrected with reference to the signal of α-methylene of THF (δ 3.58) as a standard.

(20) The chemical shift was corrected with reference to the signal of α-methylene carbon of THF-*d*₈ (δ 67.4) as a standard.

(21) The author has deposited atomic coordinates for **2a**, **2b**, and **2c** to the Cambridge Crystallographic Data Centre. The coordinates can be obtained, on request, from the Director, Cambridge Crystallographic Data Centre, 12 Union Road, Cambridge, CB2 1EZ, UK.

C₂₆H₃₆Si; space group *P*₁*n**m**a*; *a* = 14.258(3) Å, *b* = 16.029(2) Å, *c* = 9.386(2) Å; *V* = 2145.0(5) Å³; *Z* = 4; *D*_{calc} = 1.166 g/cm³; μ(Cu Kα) = 9.94 cm⁻¹; total of 1858 reflections within 2θ = 120.1° and *I* > 3σ(*I*). The final *R* factor was 4.0% (*R*_w = 4.6%). Crystal data for **2b** are as follows: C₂₆H₃₆Ge; space group *P*₁*n**m**a*; *a* = 14.291(4) Å, *b* = 16.080(3) Å, *c* = 9.380(4) Å; *V* = 2155(1) Å³; *Z* = 4; *D*_{calc} = 1.298 g/cm³; μ(Cu Kα) = 19.57 cm⁻¹; total of 1868 reflections within 2θ = 120.1° and *I* > 3σ(*I*). The final *R* factor was 4.2% (*R*_w = 4.9%). Crystal data for **2c** are as follows: C₂₆H₃₆Sn; space group *P*₁*n**m**a*; *a* = 14.922(4) Å, *b* = 16.044(2) Å, *c* = 9.370(4) Å; *V* = 2243(1) Å³; *Z* = 4; *D*_{calc} = 1.383 g/cm³; μ(Cu Kα) = 91.01 cm⁻¹; total of 1939 reflections within 2θ = 120.1° and *I* > 3σ(*I*). The final *R* factor was 4.2% (*R*_w = 5.0%). All of these structures were solved by heavy-atom Patterson methods and expanded using Fourier techniques.²² The non-hydrogen atoms were refined anisotropically. Hydrogen atoms were refined isotropically except for the methyl hydrogen of **2c**, whose positions were geometrically calculated and fixed.

VT NMR Measurements. The ¹H NMR spectrum (90 MHz) was measured for **2a** in THF-*d*₈ at the temperature range of -40 °C to 10 °C, for **2b** in THF-*d*₈ at the temperature range of -30 °C to 40 °C, and for **2c** in nitrobenzene-*d*₅ at the temperature range of -55 °C to 100 °C.

Total line-shape analyses were conducted at the five points near the coalescence temperature, and the rate constants were determined as follows: **2a**, *k* = 77 ± 10 s⁻¹ at *T* = 253.1 K; *k* = 115 ± 10 s⁻¹ at *T* = 256.2 K (coalescence temperature); *k* = 143 ± 10 s⁻¹ at *T* = 258.1 K; *k* = 225 ± 25 s⁻¹ at *T* = 263.1 K; *k* = 590 ± 60 s⁻¹ at *T* = 273.1 K; **2b**, *k* = 46 ± 4 s⁻¹ at *T* = 278.1 K; *k* = 77 ± 3 s⁻¹ at *T* = 283.1 K (coalescence temperature); *k* = 145 ± 15 s⁻¹ at *T* = 288.1 K; *k* = 210 ± 20 s⁻¹ at *T* = 293.1 K; *k* = 350 ± 50 s⁻¹ at *T* = 298.1 K; **2c**, *k* = 25 ± 3 s⁻¹ at *T* = 343 K; *k* = 37 ± 2 s⁻¹ at *T* = 348 K (coalescence temperature); *k* = 61 ± 4 s⁻¹ at *T* = 353 K; *k* = 100 ± 10 s⁻¹ at *T* = 358 K; *k* = 143 ± 20 s⁻¹ at *T* = 363 K. Activation parameters were obtained from the plot of ln *k* against 1/*T* by the conventional method.

Acknowledgment. Support of the present work by Yamada Science Foundation and by Grant-in-Aid for Scientific Research on Priority Areas (No. 06226240) from the Ministry of Education, Science and Culture, Japan is gratefully acknowledged. We also thank Professor Yasuo Hata for valuable technical advice upon X-ray crystallography. Computation time was provided by the Super Computer Laboratory, Institute for Chemical Research, Kyoto University.

Supplementary Material Available: ¹³C NMR spectra at room temperature, variable-temperature ¹H-NMR and the simulated spectra, and tables of bond lengths and bond angles of **2a–c** (9 pages). This material is contained in libraries on microfiche, immediately follows this article in the microfilm version of the journal, and can be ordered from the ACS; see any current masthead page for ordering information.

JO941830W

(22) TeXsan: Crystal Structure Analysis Package, Molecular Structure Corporation (1992).